Influence of the universal microwave background radiation on the extragalactic cosmic-ray spectrum

F. A. Aharonian
Max-Planck-Institut für Kernphysik, Saupfercheckweg 1, 69117 Heidelberg, Germany

J. W. Cronin
Enrico Fermi Institute and Department of Physics, University of Chicago, 5640 Ellis Avenue, Chicago, Illinois 60637

(Received 7 March 1994)

Features of the spectrum of the most energetic cosmic-ray protons produced by their passage through the 2.7 K universal background radiation are investigated by Monte Carlo techniques. We discuss the influence of various factors on the spectrum of protons observed at Earth with energies above 3×10^{19} eV. These factors include the shape of the initial cosmic-ray spectrum, the spatial distribution of sources, and the energy-dependent diffusion and escape of particles from a confinement region.

PACS number(s): 98.70.Sa, 98.70.Vc

I. INTRODUCTION

The current models of the origin of cosmic rays (CR's) coupled with the lack of a strong observed anisotropy suggest that the particles observed at energies $E \geq 10^{19}$ eV are most probably of extragalactic origin. If these particles are protons, their interaction with the 2.7 K universal microwave background radiation (MBR) gives rise to the "blackbody cutoff" in the spectrum at $E \geq 5\times10^{19}$ eV [1]. This remarkable spectral feature is generally considered as a signature of extragalactic CR's. The parameter characterizing the "blackbody cutoff" ($E_{1/2}$) is defined as the energy at which the differential spectrum drops to $\frac{1}{2}$ of its extrapolated value. It depends essentially on the CR diffusion time in the intergalactic medium (IGM). Even for a relatively short diffusion time $t_D \sim 3\times10^8$ yr, $E_{1/2}$ becomes less than 10^{20} eV, independent of the initial energy of the proton. If such a cutoff is not observed it may be interpreted as a result of concentration of the highest-energy CR sources within the local supercluster (LS). Similar considerations require that the cosmic-ray event observed by the Fly's Eye group at 3×10^{20} [2] must have its origin at a distance ≤ 50 Mpc. In general, however, the existing experimental data are insufficient to draw any definitive conclusions. The most concise presentation of the cosmic-ray spectrum at the highest energies is given in the review by Watson [3]. To this must be added the recent paper of the Fly's Eye group [2].

Our knowledge of the CR spectrum at highest energies will be improved in the near future, with the measurements from the 100-km^2 Akeno array [4], and the high-resolution Fly's Eye [5]. However, definitive conclusions may require detectors with a sensitivity of many 1000 km^{2}sr located in both hemispheres so that the entire sky can be observed [6]. The rather high statistics provided by these future detectors will allow accurate measurements of the absolute fluxes of CR, and also a search for possible dependence of the spectral shape on their direction. Thus, predictions of the spectral features of $\geq 10^{19}$ eV CR expected for different production and propagation models are of practical value.

With a limited data set, the observation of a sharp cutoff on a steeply falling spectrum may not have an unambiguous interpretation. For example, it may be that the original source spectrum contains that feature. The interaction of CR's with MBR has another characteristic feature: namely, a "bump" preceding the "cutoff." Observation of this feature would confirm the "blackbody cutoff." The "bump," predicted by Hill and Schramm [7], is a result of strong (exponential) dependence of the CR proton free path on energy. Protons with energy $E \geq E_{1/2}$ effectively interact with MBR due to photomeson processes, lose energy, and are accumulated in a region between 3×10^{19} eV and $\sim E_{1/2}$, where the probability of the interaction drops sharply. The formation of this "bump" is a common feature in all of the calculations including those which assume a continuous energy loss [8] even though this technique does not describe properly all aspects of the propagation [9,10]. In fact, fluctuations in the energy loss produce a much broader "bump" with lower amplitude than would be expected if the energy loss were continuous and terminating abruptly at a fixed minimum energy.

The propagation is described correctly by the kinetic transport equation with a collision integral for the photomeson processes [7,9]. While this approach permits the analysis of the general features of the spectrum, it does not provide the flexibility for the solution for a variety of practical problems. From this point of view, the Monte Carlo method has certain advantages. The goal of the Monte Carlo calculations presented here is the investigation of the profiles of the spectral features arising in the single-source and diffuse spectra of CR protons above 3×10^{19} eV during their passage through 2.7-K universal background radiation. In this paper we discuss the influence of the factors characterizing the production and propagation of extragalactic CR on the resulting CR pro-

ton spectra. These factors include the form of the source function, the spatial distribution of the CR sources, and energy-dependent conditions on the time of diffusion and escape from a confinement region. We do not consider any specific model of the CR production, but try to present the results in some general form to demonstrate the various possible effects, connected *only* with the CR proton propagation and interaction with MBR in the IGM. We limit this study by relatively nearby sources with cosmological redshifts $z \ll 1$, which allows us to neglect possible evolutionary effects connected with both MBR and CR sources. The cosmologically distant sources do not contribute much to the energy region of CR $\geq 10^{19}$ eV, which is the primary interest of this paper. The evolutionary effects have been treated in a recent paper by Yoshida and Teshima [10].

II. DESCRIPTION OF THE MONTE CARLO CALCULATIONS

The two important processes of interaction of relativistic protons with low-frequency ambient photons are (e^+e^-) pair production and photomeson production. These have been considered by many authors [8,10,11]. The inelasticity of the first process is very low ($\approx m_e/m_p$) so that the energy loss of protons is gradual. The characteristic lifetime for energy loss for this process at energies $\geq 10^{19}$ eV is $t_{\pm} = E/(dE/dt)_{\pm} \approx 5 \times 10^9$ yr [11]. Therefore this process is not an important influence on the spectrum for propagation times, $t_D \leq 10^9$ yr. For this propagation time scale we can ignore also the evolutionary effects connected with both MBR and the CR sources.

The photomeson production cross section is much smaller than the cross section of the (e^+e^-) pair production. However, because of its large inelasticity ($\geq 10\%$ energy loss in each interaction), this process is the dominant one at energies $E \geq 3 \times 10^{19}$ eV.

There is extensive data on photomeson production. For single-meson production the angular distributions have been well measured. With the onset of multiple meson production the data are less complete as far as the details of the final states, but the total cross sections are well measured. We have used the compilation of the DESY e^+e collider HERA and COMPAS groups for the input data for our calculations [12]. Most important are the total cross sections and the ratio of the charge exchange to the charge retention process. The latter are important at energies where the neutron decay length becomes comparable or longer than the interaction length. We have compared the result of our calculations for the case where one assumes an isotropic angular distribution in place of the measured one. We have also compared results for various plausible assumptions of the inelasticity and its distribution in the regime of multiple meson production. None of these refinements make a significant difference over the assumption that the total cross section always corresponds to a single pion produced isotropically. Yoshida and Teshima have reached the same conclusion [9]. This simplification would be unacceptable if we also were concerned with the subsequent propagation of the decay products of the pions, such as γ rays and neutrinos.

To simulate the propagation of protons (and neutrons) via intergalactic medium, we divide the given propagation distance (or time) into thin layers, typically $\delta = 0.1-1$ Mpc, where the interaction length of highest energy cosmic rays, λ_p, is always large compared to δ. This technique, while it is more computationally intensive, has an advantage over the standard method in which the interaction path is chosen by means of a random number. It provides a simple way to investigate the propagation of CR in the general case of the energy-dependent diffusion time in the IGM. It also provides a simple procedure to take into account continuous energy losses due to pair production, as well as the evolutionary effects if such effects are important.

We first show the general features of the propagation of protons in the MBR which allows one to understand qualitatively the various specific cases we treat in the paper. In Fig. 1(a), we plot the mean energy of protons as a function of propagation distance. After a distance of ≈ 100 Mpc, or propagation time of $\approx 3 \times 10^8$ yr, the mean energy is essentially independent of the initial energy of the protons, and that energy is less than 10^{20} eV. Energies in excess of 10^{20} eV correspond to a propagation time $\leq 3 \times 10^8$ yr. In Fig. 1(b), we plot the ratio of the rms energy fluctuations to the mean energy as a function of propagation distance. These fluctuations are very significant in the range 10–100 Mpc. The fluctuations are important in determining the more detailed features of the spectrum below the cutoff such as the "bump" referred to above.

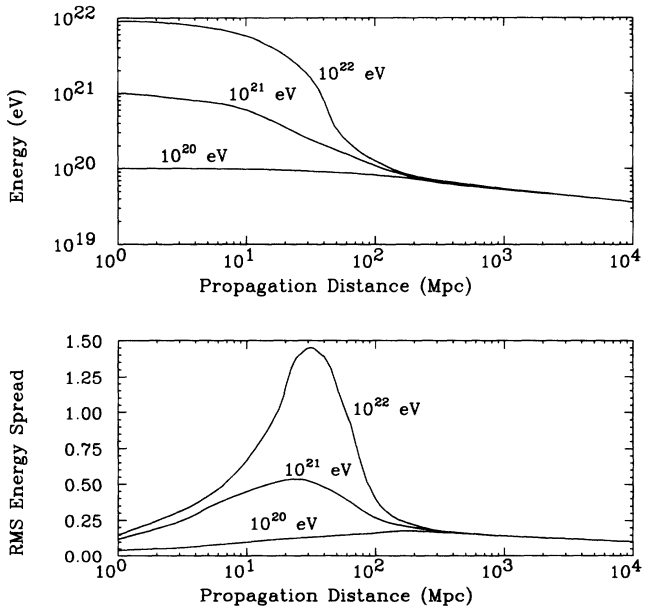

FIG. 1. (Above) Mean energy as a function of propagation distance (time) for protons of indicated initial energies. (Below) Ratio of rms fluctuations of energies to mean energy as a function of propagation distance (time) for the indicated initial energies.

III. RESULTS

The observed energy spectrum of high-energy protons ($E \geq 3\times10^{19}$ eV) produced in extragalactic sources depends on (i) the spatial distribution and character of propagation of CR in the intergalactic magnetic fields, (ii) the energy spectrum of accelerated particles injected in the IGM, (iii) energy losses due to interactions with the intergalactic photon fields, and (iv) the time history (evolution) of sources. All these factors are model dependent and rather uncertain. But as far as the highest-energy part of the spectrum is concerned, the bulk of particles is contributed by relatively nearby sources, the propagation time which does not exceed 3×10^8 yr. This circumstance removes the most speculative ambiguity associated with possible cosmological evolution of sources. In addition, for relatively close sources we can neglect interactions of CR protons with other intergalactic background fields such as infrared photons which influence principally the spectrum below the energies of interest [13]. Since the cross sections of the photomeson processes in the appropriate energy region [12], and the energy spectrum of MBR [14] have been well measured, the uncertainties relate to points (i) and (ii). In the following sections we discuss a variety of possibilities that result from different assumptions concerning points (i) and (ii). There are cases where quite different assumptions lead to nearly identical results so that even with good statistics the ambiguities of interpretation will persist.

A. The single-source power-law injection spectrum

There is direct as well as indirect evidence that the spectra of accelerated particles have a power-law behavior in a wide energy region. The spectrum is represented by

$$I_0(E) \propto E^{-\Gamma}, \quad E_1 \leq E \leq E_2 . \tag{1}$$

The spectral index Γ, as well as the lower and upper limits E_1 and E_2, generally are determined by the ratio of the acceleration rate to the energy-loss rate. Power-law spectra are predicted by most acceleration mechanisms, e.g., acceleration of CR's by shock waves. Thus, it seems reasonable that the power-law *injection* spectra are usually expected also for the highest-energy cosmic rays, though at present there is no conclusive experimental evidence for the spectral shape of particles above 3×10^{19} eV. Moreover, if these particles have an extragalactic origin, the interactions with MBR can change dramatically the original spectral shape of accelerated particles injected in the IGM. We define a *modification factor* $f(E)$ given by

$$f(E)=\frac{I_p(E)}{I_0(E)} , \tag{2}$$

where $I_0(E)$ is the injected spectrum and $I_p(E)$ is the spectrum as modified by the MBR. In Fig. 2, we plot $f(E)$ calculated for $E_1=0$, $E_2=10^{21}$ eV, and for different values of spectral index Γ and CR propagation path L (in case of rectilinear propagation L corresponds to the distance to the source, $L=R$). These results are in general

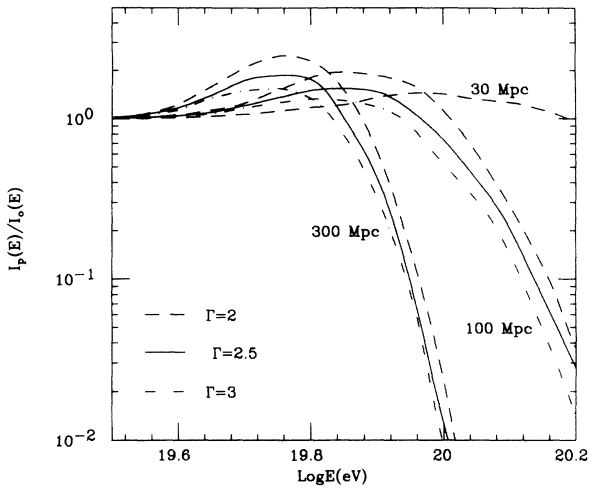

FIG. 2. The modification factor $f(E)=I_p(E)/I_0(E)$ of the single-source energy spectra of protons, calculated for different values of the CR propagation distance L and power-law index of the initial spectrum Γ, as indicated. In this and subsequent figures, log represents the logarithm with base 10.

agreement with single-source spectra calculated earlier by Monte Carlo simulations [10] and by solving the transport kinetic equation [9]. Both of these techniques predict a much smaller "bump" than the continuous energy-loss approximation [7]. The amplitude of the "bump" is a factor of 2.5 in the case of very hard injection spectrum with $\Gamma=2$, and is a factor of 1.5 in the case of $\Gamma=3$. A harder spectrum produces a more significant "bump" since the number of high-energy protons interacting with MBR is significantly larger. It is conventional to plot the spectrum, weighted by E^3, to emphasize small changes in the slope of the spectrum. The recent Fly's Eye analysis of the CR spectrum at energies $\leq 3\times10^{19}$ eV [2], where distortion of the initial spectrum due to interactions with MBR becomes negligible, indicates a harder injection spectrum than $\propto E^{-3}$. We note that

$$E^3 I_p(E) \propto f(E) E^{3-\Gamma} , \tag{3}$$

hence, for an injection spectrum index, $\Gamma < 3$, the increase of the function $E^3 \times I(E)$ is provided not only by the real physical "bump," due to the MBR, but also due to the rise of the function $E^{3-\Gamma}$. Therefore, a possible experimental indication on the maximum in the function $E^3 \times I(E)$ at $E \geq 3\times10^{19}$ eV [13], is not sufficient evidence for a real "bump" in the spectrum. In addition the energy resolution of the detector will have a significant influence on the observability of a "bump." The effect of energy resolution is discussed below.

For sources not too distant ($\sim$30 Mpc), the shape of the spectrum of cosmic rays, as observed, depends strongly on the upper bound of the injection spectrum E_2. An upper bound E_2 in the initial spectrum should exist in the case of any reasonable mechanism of particle acceleration, in particular due to insufficient magnetic confinement of highest-energy particles in the acceleration region (see, e.g., [15]). Unfortunately, the blackbody

"cutoff" masks E_2, which makes the experimental probing of this very important parameter difficult. Some information about the upper limit is contained, in principle, in the highest-energy part of the observed spectrum. For a source distance of 30 Mpc this is demonstrated in Fig. 3 for different values of E_2. In the energy region $E > 10^{21}$ eV the mean free path of protons in the MBR becomes almost energy independent, which allows one to find a simple analytic solution for $f(E)$ from the kinetic transport equation [9]:

$$f(E)=\frac{I(E)}{I_0}\cong\exp\left[-\frac{\Gamma-1}{\Gamma}\frac{t}{\tau_0}\right], \tag{4}$$

where $t=L/c$ is the propagation time and $\tau_0=(\sigma_0 c n_{\rm ph})^{-1}$ is the mean interaction time; $\sigma_0\approx 1.3\times10^{-28}$ cm^2 is the total p-γ photoproduction cross section at high energies, and $n_{\rm ph}\sim 400$ cm^{-3} is the total MBR photon density with an average energy $\simeq 6\times10^{-4}$ eV. So, in the case of $E_2\to\infty$, the spectrum of protons formed in the IGM repeats the form of the injection spectrum, but with an amplitude lower by a factor of $\approx\exp\{[(\Gamma-1)/\Gamma](t/\tau_0)\}$. Since $\tau_0\times c\approx 6$ Mpc, the detection possibility of this part of the spectrum, even for relatively nearby sources, is strongly limited by statistics. The technique outlined above can only be successful if a source can be found, since over the whole sky it is unreasonable to expect the sources to be at a uniform distance. Moreover, for reasonable values of E_2, namely $E_2\le 10^{22}$ eV, the spectrum becomes steeper than predicted from Eq. (4).

As we see from Fig. 3, the highest-energy part of the spectrum beyond the blackbody "cutoff" is not totally abrupt; its shape depends strongly on the value of E_2. The latter affects also the spectral shape below the "cutoff." In particular, for $E_2=10^{20}$ eV, $E_{1/2}$ occurs at lower energies than for $E_2\ge 10^{21}$ eV. In addition, for $E_2=10^{20}$ eV the "bump" practically disappears. Thus, measurement of the energy spectrum in the region of the "bump" and "cutoff" can provide, in principle, some indirect information about E_2, but in practice, it would be difficult to make definitive conclusions. First, the moderate energy resolution of detectors and limited statistics at highest energies may not allow sufficiently precise spectrum measurements as discussed below. Second, spectra such as shown in the curve labeled 1 in Fig. 3, i.e., with "cutoff" at $E<10^{20}$ eV but with negligible "bump," could be formed in other models, for example, in the case of diffuse (many-source) models with more or less homogeneous distribution of CR sources in the Universe. In subsequent calculations we will use the value $E_2=10^{21}$ eV.

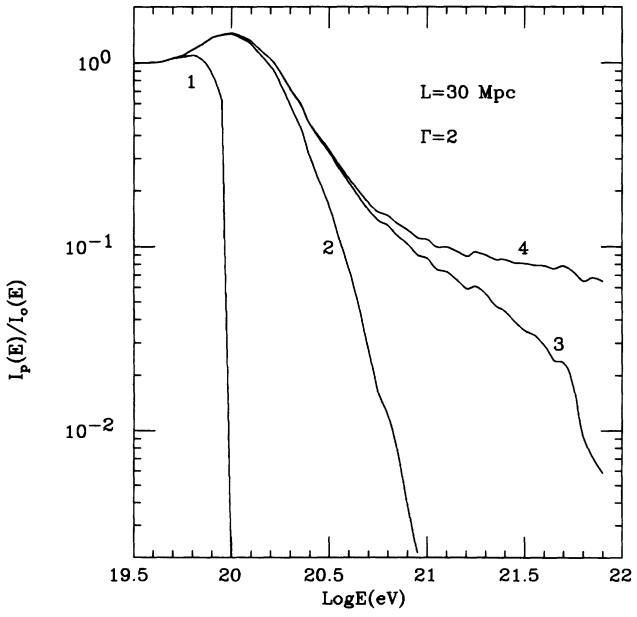

FIG. 3. The modification factor of the single-source energy spectra of protons for $L=30$ Mpc, and for different high-energy upper limits ("ends") of the initial power-law ($\Gamma=2$) spectrum, E_2: (1) $E_2=10^{20}$ eV; (2) $E_2=10^{21}$ eV; (3) $E_2=10^{22}$ eV; (4) $E_2=10^{23}$ eV. $L=30$ Mpc. Note that the "wiggles" are indicative of the Monte Carlo statistics.

B. The diffuse spectra

The single-source spectra (S spectra) in Fig. 2 correspond to fixed CR propagation path lengths which, in practice, may be realized when the bulk of CR is contributed by a *single* source or by several sources located in the same region (e.g., by galaxies of the Virgo cluster). In the case of *many* extragalactic sources having broad distribution in distances and luminosities one has to integrate the contribution of all sources. The solution of the problem becomes very simple if we assume that CR sources with comparable luminosities populate the Universe homogeneously; this is called the *universal* model (UM) of CR.

Because of the superposition of contributions of distributed sources, the spectral features of diffuse spectra (D spectra) are smoother than S spectra. The "bumps" from sources at different distances do not amplify each other, since they appear at different energies. Thus, the resulting "bump" is less pronounced, and in the idealized case of the UM it disappears altogether [8,9]. The high-energy tails of D spectra beyond "cutoff" are also less steep than in S spectra. The diffuse spectra, presented in Fig. 4, correspond to homogeneous distribution of sources within a sphere with radius $R=\kappa c t_{\rm max}$, where c is the speed of light, and the coefficient κ takes into account a possible delay of the arrival time of particles due to diffusion in the intergalactic magnetic fields.

In fact, CR sources are not necessarily distributed in space homogeneously. This adds a new uncertainty in the expected shape of the spectrum detected by the observer, since the distribution of CR sources in distances and luminosities can only phenomenologically be taken into account. The D spectra corresponding to three different distributions of CR sources are shown in Fig. 5. Hereafter in the figures we present the differential spectra in the form $dI/d\log_{10}E$, with a normalization $I_0(\ge E_0)=1$, which gives the relative number of particles at the given narrow interval of $\ln E$. The curves 1 and 2 in Fig. 5 correspond to a homogeneous distribution of

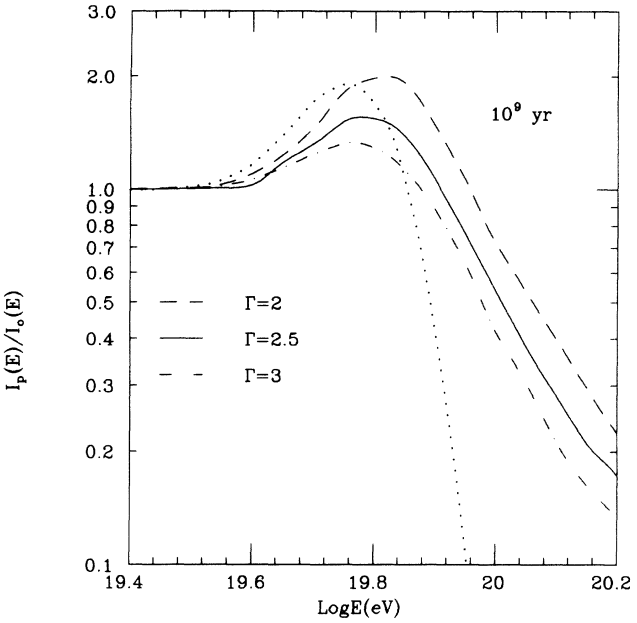

FIG. 4. The modification factor for diffuse (many-source) spectra of protons, calculated for a homogeneous distribution of the CR sources. The maximum propagation time, $\tau_{max}=10^9$ yr and the power-law index of the initial spectrum, $\Gamma=2$; 2.5; and 3. For comparison, the single-source spectra (dotted curve) for $\Gamma=2.5$ and propagation time $\tau=10^9$ yr are also shown.

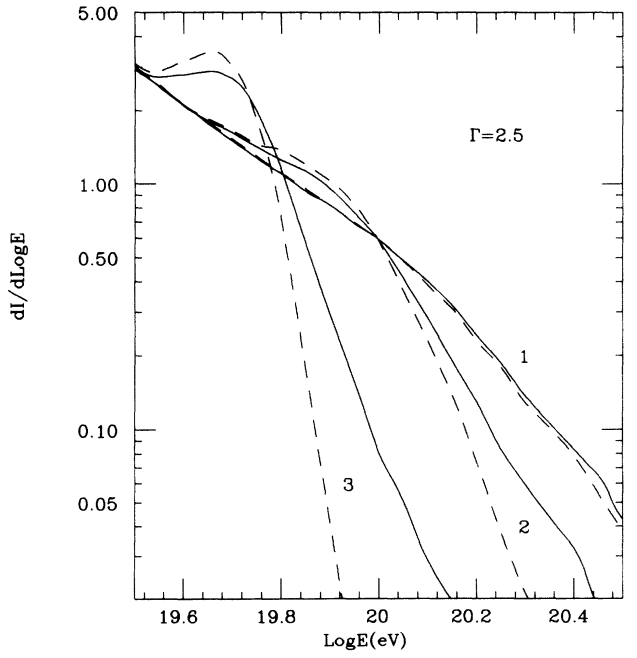

FIG. 5. The diffuse (many-source) spectra of protons, calculated for different assumptions on the spatial distribution of the CR sources. Solid curves: homogeneous distribution of sources between $L_{min}=0$ and (1) $L_{max}=30$ Mpc; (2) $L_{max}=100$ Mpc; (3) $L_{max}=1000$ Mpc. Dashed curves: (1) homogeneous distribution of sources between $L_{min}=5$ Mpc and $L_{max}=30$ Mpc; (2) homogeneous distribution of sources between $L_{min}=30$ Mpc and $L_{max}=100$ Mpc; (3) nonhomogeneous distribution of sources between $L_{min}=0$ and $L_{max}=1000$ Mpc for $\dot{W}(R)\propto R^2$. The initial power-law index: $\Gamma=2.5$; normalization: $I_0(\geq 3\times 10^{19}\text{ eV})=1$.

sources between L_{min} and L_{max}. They show that at $L_{min}\ll L_{max}$ the observed spectrum depends on L_{max}, but rather weakly on L_{min}. However, in the case of $(L_{max}-L_{min})/L_{max}\ll 1$ the D spectrum obviously should be rather similar to the S spectrum. The "S"-like spectrum arises also in case of a strong increase of the CR source injection power with distance (or time), e.g., $\dot{W}_{CR}\propto R^2$. As seen in Fig. 5, the spatial distributions of CR sources $\dot{W}_{CR}(R)\propto$ const and $\dot{W}_{CR}(R)\propto R^2$ give noticeably different D spectra.

The difference of formation of S and D spectra can be demonstrated clearly in the case of monoenergetic injection of CR into the IGM as shown in Fig. 6. For monoenergetic particles with $E_0\geq 10^{20}$ eV and distances to the source $R\gg\lambda_p\sim 10$ Mpc, the interaction with MBR is so effective that it leads to formation of a Gaussian-like S spectrum, independent on the initial energy of particles. The D spectrum is not only broader than the S spectrum, but it contains also the noninteracting part, $\approx 5\%$ of all particles, coming from nearby sources. The common general feature of both S and D spectra is their general approximately Gaussian-like shape which is the result of the absence of low-energy particles in the injection spectrum. Obviously, this type of spectra appears not only in the case of monoenergetic injection, but also for power-law injection spectra with the low-energy limit at $E_1\geq 10^{20}$ eV. The strong dependence of the resultant spectra on the value of E_1 is shown in Fig. 7. The case of a monoenergetic injection is unreal-

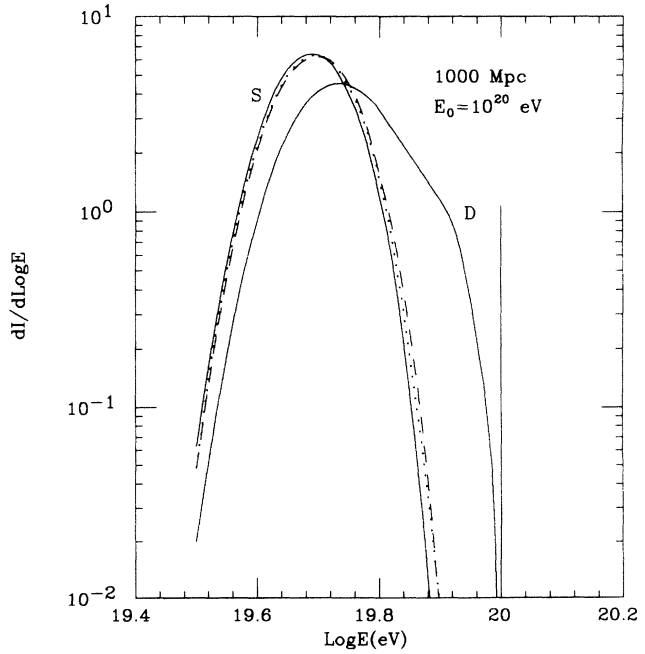

FIG. 6. The single-source (S) and diffuse (D) energy spectra for the initial monoenergetic spectrum of particles with $E_0=10^{20}$ eV, calculated for $L_s=10^3$ Mpc and $L_{max}=10^3$ Mpc, respectively. The single-source spectra for $E_0=10^{21}$ eV (dotted curve) and $E_0=10^{22}$ eV (dashed curve) are also shown. Normalization: $I_0(E_0)=1$. The vertical line at 10^{20} eV represents the 5% of the D spectrum that does not interact.

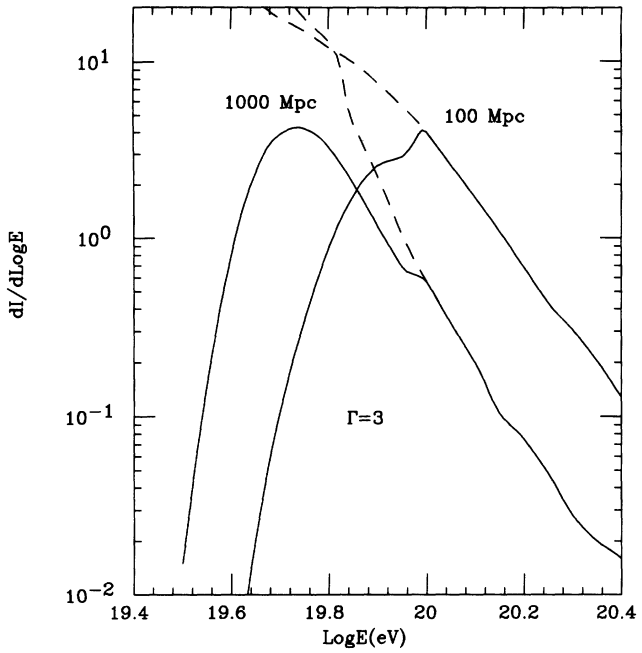

FIG. 7. The diffuse energy spectrum for the initial power-law spectrum of particles ($\Gamma=3$) with (solid curves) and without (dashed curves) a low-energy cutoff at $E_1=10^{20}$ eV. The values of the maximum CR propagation length, 10^2 Mpc and 10^3 Mpc, are indicated at curves. Normalization: $I_0(\geq 10^{20}\text{ eV})=1$ for the injected spectrum.

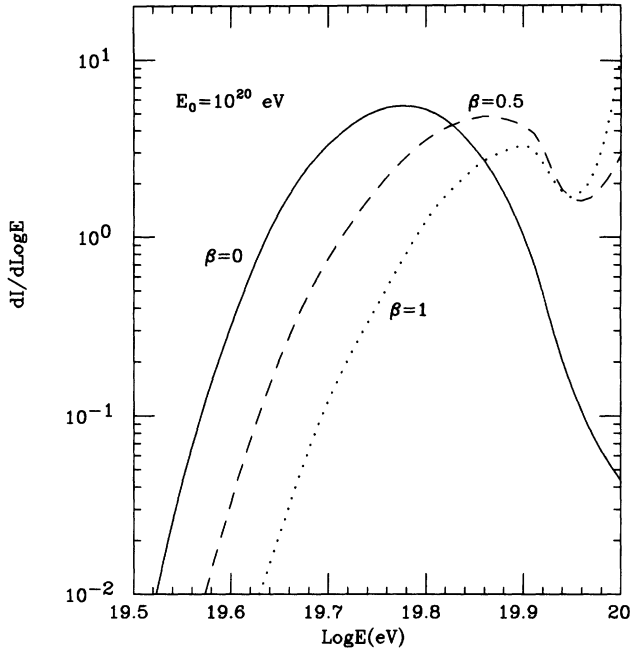

FIG. 8. The single-source spectra of protons for the initial *monoenergetic* spectrum ($E_0=10^{20}$ eV) and energy-dependent CR propagation distance: $L(E)=300(E/10^{19}\text{ eV})^{-\beta}$ Mpc. The values of the parameter $\beta=0$; 0.5; 1 are indicated adjacent to the curves. The curves are normalized to one primary particle.

istic but it gives a clear understanding of the formation of the resultant spectra in the IGM when there is a power-law injection spectrum with high value of $E_1\sim 10^{20}$ eV which could actually exist. For example, the low-energy cutoff may be the result of the magnetic confinement of protons in the source(s), e.g., in clusters of galaxies. It is interesting to note that even in the case of the total confinement of protons in clusters with size $R\geq 1$ Mpc, their partial escape, namely, the leakage of the high-energy tail, is possible via neutrons, produced at interactions with MBR and possibly, with other photon fields inside the source. This case is discussed below.

C. Energy-dependent propagation

All calculations presented above correspond to the rather idealized situation where it is assumed that the propagation of particles is essentially energy independent. In fact, the diffusion coefficient of the particle propagation generally depends on energy. The distribution of random field scales in the IGM is quite uncertain; therefore, calculations of energy-dependent diffusion coefficient $D(E)$ can be done only by empirical models of CR propagation [16,17]. These models predict the dependence $D(E)\propto E^{\beta}$ with $\beta\sim 0.3-1$. They may be tested by forthcoming experiments with giant arrays, primarily by measurements of anisotropy of the angular distribution of highest-energy particles. In addition, information on $D(E)$ is also contained in the energy spectrum. In Figs. 8 and 9, we show the energy spectra of protons

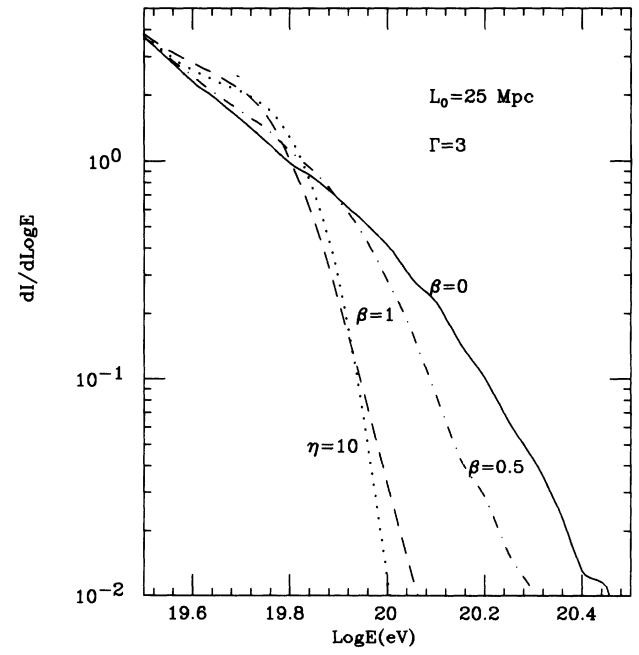

FIG. 9. The single-source spectra of protons for energy-dependent CR propagation path: $L(E)=L_0(E/10^{21}\text{ eV})^{-\beta}$; $L_0=25$ Mpc. The values of the parameter β are indicated at curves. The dotted curve corresponds to the case of $\beta=0$, but $L=\eta\times L_0$; $\eta=10$. The initial spectrum is power law with $\Gamma=3$. Normalization: $I_0(\geq 3\times 10^{19}\text{ eV})=1$.

from a single source with fixed distance R, but for different propagation lengths before reaching the observer, $L(E) \propto R^2/D(E) \propto E^{-\beta}$. The case of monoenergetic initial spectrum, $E_0 = 10^{20}$ eV and $L(E) = 300(E/10^{19}\ \text{eV})^{-\beta}$, Mpc is presented in Fig. 8. It illustrates a dramatic influence of the parameter β on formation of the spectrum. For $\beta = 0$, i.e., constant propagation length with $L(E) = 300$ Mpc, a Gaussian-like spectrum is formed with a negligible number of particles with an energy near 10^{20} eV. But for $\beta = 0.5$, and especially $\beta = 1$, when high-energy particles spend much less time to reach the observer, many particles survive with energies close to 10^{20} eV. In Fig. 9, we show the case of the initial power-law spectrum with $\Gamma = 2$. The propagation length $L(E) = 25(E/10^{21}\ \text{eV})^{-\beta}$ used in this case may be interpreted as rectilinear propagation of particles from the source at distance $R = 25$ Mpc at energies $\geq 10^{21}$ eV, but with delay ($\propto E^{-\beta}$) in arrival time at lower energies. This scenario may be realized, probably, in the model of particle production in the Virgo cluster. The difference between $\beta = 0$ and 1 is so strong, that the two cases may be distinguished by measurements of the energy-dependent angular distribution in future experiments if Virgo proves to be a source.

Another possible scenario is the case of particles partially confined in some region, e.g., in our supercluster, with an escape time, depending on energy. The diffuse spectra of protons for an observer *inside* the confinement region are shown in Fig. 10. In the calculations we took, for the escape time, $\tau_{\text{esc}} = 10^9(E/10^{19}\ \text{eV})^{-s}$ yr, and for the duration of injection $\Delta t = 3 \times 10^9$ yr which could be interpreted as "active phase," i.e., a nearly constant CR injection rate in the intercluster region during the last 3×10^9 yr. Note that at $\tau_{\text{esc}} \gg \Delta t$ a typical D spectrum is formed. But in the case of $\tau_{\text{esc}} \leq \Delta t$, the escape losses become very important, leading to a decrease of the absolute flux of particles for an observer inside the confinement region. The escape losses, together with energy losses due to interactions with MBR, determine the spectral shape of protons. The "bump" and "cutoff," characterizing interactions with MBR, survive in the spectrum until the interaction time is comparable with escape time. They gradually disappear at $\tau_{\text{esc}} \leq t_{\text{int}}$, when escape losses dominantly determine the spectrum of protons, transferring the initial $E^{-\Gamma}$ spectrum to the softer, $I(E) \propto E^{-\Gamma - s}$, spectrum.

Even a total magnetic confinement of protons within sources cannot prevent a partial escape of particles via secondary neutrons [18]. The minimum energy of neutrons escaping the source, and correspondingly the low-energy cutoff in the spectrum of protons, produced at decays of neutrons outside of the source with linear size scale l, roughly may be estimated as $E \approx m_N c l/\tau_N \approx 10^{20}(l/1\ \text{Mpc})$ eV if one assumes that the neutrons produced in interaction with the MBR do not interact before escaping the source. This approximation remains correct even for highest-energy neutrons, provided the source size does not exceed significantly the mean-free-path length of nucleons, $\lambda_N \approx (\sigma_{N\gamma} n_{\text{ph}})^{-1} \sim 5$ Mpc. Thus, for models with total confinement of CR in clusters of galaxies with typical size $l \sim 1$ Mpc, we would expect

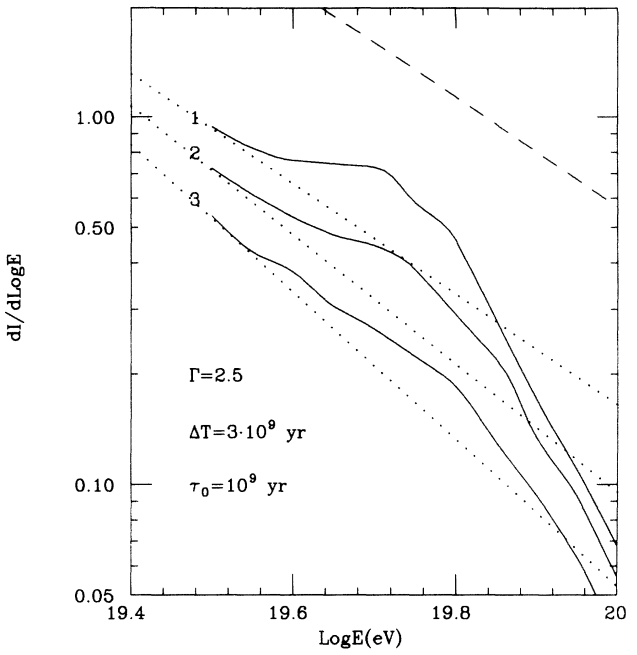

FIG. 10. The diffuse spectra of protons inside the confinement region for the energy-dependent time of escape from the confinement region: $\tau = \tau_0(E/10^{19}\ \text{eV})^{-s}$ eV; $\tau_0 = 10^9$ yr. Curves 1, 2, and 3 correspond to $s = 0$, 0.25, 0.5, respectively. The dashed curve is the initial spectrum with power-law index of $\Gamma = 2.5$; normalization: $I_0(\geq 3 \times 10^{19}\ \text{eV}) = 1$. The integration time (duration of injection) $\Delta t = 3 \times 10^9$ yr. The dotted curves correspond to the diffuse spectra, formed due to the particle escape from the confinement region without the effect of the MBR.

an injection spectrum of protons to the intercluster region with a low-energy cutoff near 10^{20} eV. The Monte Carlo calculations for the energy spectra of protons, established inside and outside of the source with a mean size $\bar{l} = 1$ Mpc are presented in Fig. 11. Though the flux of particles above 10^{20} eV, established outside of the source, exceeds the flux inside the confinement region, the total number of escaping neutrons is too small, and they do not have much effect for $\bar{l} \geq 1$ Mpc on formation of the spectrum inside the confinement region. However, this effect leads to the injection of protons into IGM with a nearly power-law spectrum with low-energy cutoff at $E_1 \sim 10^{20}$ eV. A Gaussian-like resultant spectrum (as the spectrum shown in Fig. 7), will occur if the bulk of highest-energy cosmic rays are contributed by clusters or superclusters of galaxies.

IV. DISCUSSION

The Monte Carlo approach for study of formation of the highest-energy proton spectrum provides a rather simple but quite correct and convenient way to investigate the influence of different parameters, characterizing the cosmic-ray sources and diffusion of particles in the IGM. The presented results show that the problem of the spectrum formation in the field of MBR cannot be brought to the simple case of a production of a "bump" and "cutoff." These spectral features, arising due to pho-

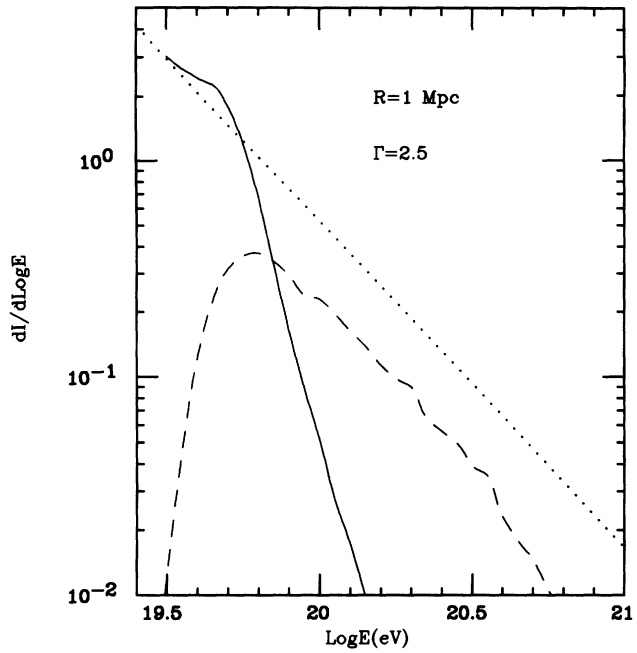

FIG. 11. The energy spectrum of protons, established inside (solid curves) and outside (dashed curves) of the source due to interactions with MBR and escape of neutrons from the source. The initial power-law spectrum is shown by the dotted curve. The integration time $\Delta t = 3 \times 10^9$ yr; the escape time of charged particles (protons), $\tau = \infty$. The mean size of the source $\bar{l} = 1$ Mpc.

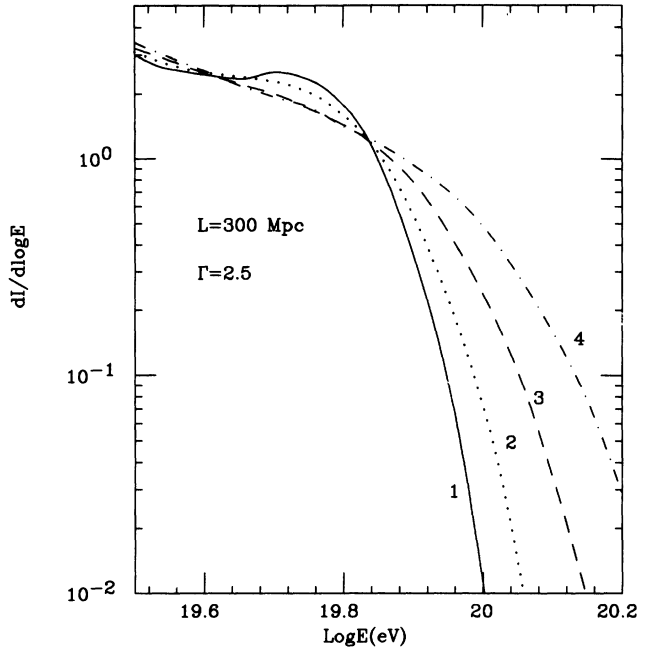

FIG. 12. The single-source spectra of protons after correction for the energy resolution of the detector. $L = 300$ Mpc; $\Gamma = 2.5$. Curves 1, 2, 3, and 4 correspond to the energy resolution $\sigma = 0$, 0.15, 0.30, 0.50, respectively.

tomeson processes at interactions with MBR, contain certain information about spatial distribution of cosmic-ray sources. However, the possible *energy-dependent* diffusion of particles in the IGM makes the unambiguous extraction of this fundamental information rather difficult. Moreover, the resultant spectrum strongly depends on the injection spectrum, in particular, on both its low- and high-energy cutoffs. The high-energy cutoff E_2 in the primary spectrum should certainly exist due to limited efficiency of the acceleration; for typical extragalactic sources the upper limit is estimated to be between 10^{20} and 10^{22} eV. The low-energy cutoff in the spectrum of particles, E_1, could be the result of partial or total magnetic confinement of accelerated particles in sources. In the last case the escape of the high-energy tail of the production spectrum is possible via secondary neutrons. For clusters of galaxies as a source of highest-energy cosmic rays, the neutron-escape mechanism gives typically $E_1 \sim 10^{20}$ eV.

The spectrum below $E \leq 3 \times 10^{20}$ eV is insensitive to values of $E_2 \geq 10^{21}$ eV. The values of $E_2 \leq 10^{21}$ eV shift the blackbody "cutoff" to lower energies and make the "bump" weaker. The low-energy cutoff in the injection spectrum, which becomes important at $E_1 \geq 10^{20}$ eV, results in the Gaussian-like spectrum, formed in the IGM. This specific shape of the spectrum is saved even in case of strong energy-dependent diffusion of particles in the IGM.

The spatial distribution of sources, the spectral shape of particles injected in the IGM, the energy-dependent diffusion, etc., make the problem of formation of the spectrum of highest-energy cosmic rays a very interesting one which involves many different aspects of high-energy astrophysics. However, the combination of these factors predicts a wide range of possible spectra of cosmic rays reaching the observer, which makes the unambiguous ex-

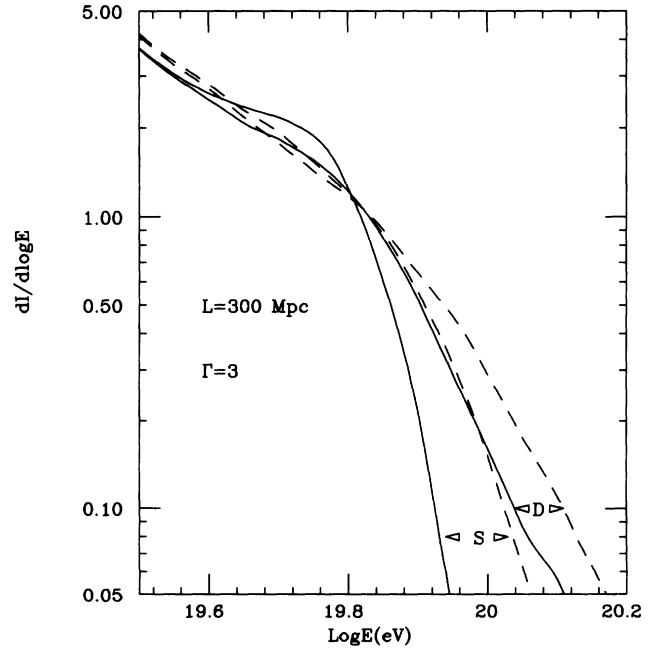

FIG. 13. The single-source (S) and diffuse (D) spectra of protons without (solid curves) and with (dashed curves) correction to the energy resolution of the detector. $L = 300$ Mpc; $\Gamma = 3$, and $\sigma = 0.3$.

traction of the fundamental information on distribution of CR sources very difficult. It requires rather precise energy measurements with small statistical errors. The spectral features of the primary spectrum are noticeably distorted due to limited energy resolution of detectors. This is clearly seen in Fig. 12, where the spectrum of protons from the source at distance 300 Mpc is presented before and after correction to the energy resolution of a detector. We see that for energy resolution of detector $\leq 10\%$ the spectrum still retains its general features, but a detector with energy resolution $\geq 30\%$ strongly distorts the primary spectrum. In particular, the "bump" totally disappears. Note, that because of the monotonically decreasing primary spectrum, the limited energy resolution "works" in one direction, namely, "shifting" low-energy particles from the "bump" region to the "cutoff" region. If uncorrected it could lead to a wrong conclusion about the model of propagation of cosmic rays. For example, for a typical 30% energy resolution for the detector the single-source spectrum is transformed to a spectrum similar to a diffuse one. This is shown in Fig. 13. Therefore, the reconstruction of the primary spectrum requires good knowledge of the (energy-dependent) response of detectors which in principle can be obtained from a combination of different kinds of detectors measuring different components of atmospheric showers, and therefore providing cross calibration of relevant characteristics. The second crucial point is the sufficient statistics of detected events, which will require detectors with acceptance of 10^4 km^2 sr or more.

ACKNOWLEDGMENTS

The major part of the work of F.A.A. was done during his visit to The University of Chicago. F.A.A. is grateful to the members of the CASA group for warm hospitality and for the financial support of Mrs. Betty C. Lewis. This work was supported by the National Science Foundation.

[1] K. Greisen, Phys. Rev. Lett. **16**, 748 (1966); G. T. Zatsepin and V. A. Kuz'min, Pis'ma Zh. Eksp. Teor. Phys. **4**, 114 (1966) [JETP Lett. **4**, 78 (1966)].

[2] D. J. Bird *et al.*, Phys. Rev. Lett. **71**, 3401 (1993).

[3] A. A. Watson, in *12th European Cosmic Ray Symposium on Solar and Galactic Cosmic Rays,* Nottingham, England, July 1990, edited by P. R. Blake and W. F. Nash [Nucl. Phys. B (Proc. Suppl.) **22B**, 116 (1991)].

[4] N. Nagano and M. Teshima, in *International Workshop on Techniques to Study Cosmic Rays with Energies Greater than* 10^{19} *eV,* edited by J. Cronin, A. A. Watson, and M. Boratav [Nucl. Phys. B (Proc. Suppl.) **28B**, 28 (1992)].

[5] S. C. Corbató *et al.*, in *International Workshop on Techniques to Study Cosmic Rays with Energies Greater than* 10^{19} *eV* [4], p. 36.

[6] J. W. Cronin, Nucl. Phys. B (Proc. Suppl.) **28B**, 213 (1992).

[7] C. T. Hill and D. N. Schramm, Phys. Rev. D **31**, 564 (1985).

[8] V. S. Berezinsky and S. I. Grigor'eva, Astron. Astrophys. **199**, 1 (1988).

[9] F. A. Aharonian, B. L. Kanevsky, and V. V. Vardanian, Astrophys. Space Sci. **167**, 93 (1990).

[10] S. Yoshida and M. Teshima, Prog. Theor. Phys. **89**, 833 (1993).

[11] F. W. Stecker, Phys. Rev. Lett. **21**, 1016 (1968); G. Blumenthal, Phys. Rev. D **1**, 1596 (1970).

[12] HERA and COMPAS Groups, Compilation of Cross-Sections IV, CERN-HERA 87-01 (CERN, Geneva, 1987).

[13] J. L. Puget, F. W. Stecker, and J. H. Bredekamp, Astrophys. J. **295**, 638 (1976).

[14] J. C. Mather *et al.*, Astrophys. J. **354**, L37 (1990).

[15] A. M. Hillas, Annu. Rev. Astron. Astrophys. **22**, 435 (1984).

[16] V. S. Berezinsky *et al.*, *Astrophysics of Cosmic Rays* (North-Holland, Amsterdam, 1991).

[17] M. Giler, J. Wdowczyk, and A. W. Wolfendale, J. Phys. G **6**, 1561 (1980).

[18] A. W. Wolfendale and J. Wdowczyk, J. Phys. A **9**, L197 (1976).